THE JOURNAL OF PHYSICAL CHEMISTRY C

Article

pubs.acs.org/JPCC

# Initial Growth Kinetics of Luminescent Quantum Clusters of Silver within Albumin Family Protein Templates

Kamalesh Chaudhari[†,‡] and Thalappil Pradeep*[,‡]

[†]Department of Biotechnology and [‡]DST Unit of Nanoscience (DST UNS) and Thematic Unit of Excellence (TUE), Department of Chemistry, Indian Institute of Technology Madras, Chennai 600 036, India

Supporting Information

**ABSTRACT:** We probed the initial growth kinetics of luminescent quantum clusters of silver (AgQCs) within two albumin family proteins, bovine serum albumin (BSA) and ovalbumin (Ova). Shorter time scale (seconds to minutes) growth of AgQCs monitored using real time photoluminescence spectroscopy has shown that, at lower concentrations of $Ag^+$, only unstable QCs were formed. The major role of basic pH in the synthesis was not only to facilitate $Ag^+$-BSA conjugation but also to provide well dispersed medium for controlled nucleation of QCs. Increase in the concentration of $NaBH_4$ affects growth kinetics greatly and leads to increase in the growth rate of AgQCs; but for $NaBH_4$ concentrations higher than the optimum value, growth rate becomes constant. Precise measurements have shown that excitation and emission of AgQCs exhibit linear red-shift with the increasing concentration of $NaBH_4$ whereas protein excitation remains constant. Similar results were observed for both the proteins, Ova and BSA. We believe that various insights provided by this study will be helpful for further improvements in the synthetic methodology and applications of protein protected AgQCs.

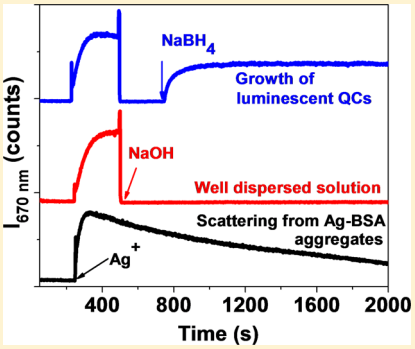


## INTRODUCTION

Protein protected luminescent noble metal quantum clusters (NMQCs@protein) have found interesting applications in the recent past.[1−7] NMQCs@protein can be synthesized using various metal ions such as copper, mercury, gold, silver, etc.[8−10] NMQCs@protein are biocompatible due to their bulky protein ligands and lower metal content.[4,11,12] Apart from this, protein ligands can be easily conjugated to drug molecules and can be targeted to cancer cells for imaging and therapy applications.[4,11,13] Photoluminescence (PL) properties of NMQCs@protein have been demonstrated to be useful for sensing amino acids.[14] In the past, NMQCs@protein have been used for the detection of post-translation modification of enzymes and determination of the activity of protease enzymes.[15,16] Studies have shown that intracellular changes in the properties of NMQCs@protein can be used to sense and monitor the activity of various analytes.[10,17] Most of these applications are based on photoluminescence of clusters. Such luminescence has been found to be stable at biological pH[18] and it is possible to tune the same by changing multiple synthetic parameters, such as pH, concentrations of reducing agent, etc.[19−23] For example, Kawasaki et al. and Guèvel et al. have demonstrated the dependence of AuQC synthesis on pH of the reaction.[19] It was found that growth of smaller clusters can happen at lower pH, whereas larger clusters can be synthesized at basic pH. Synthesis of NMQCs@protein was demonstrated using bovine serum albumin (BSA), lactoferrin, lysozyme, insulin and multiple other proteins.[2,4,18,24] Variety of synthetic methodologies have been developed for the synthesis of protein template AuQCs and AgQCs.[21,24−26] Synthetic methodologies for AuQCs and AgQCs have some basic differences. This is because, gold can be reduced by tyrosine residues of proteins at basic pH but due to lower reduction potential of silver, it requires a stronger reducing agent such as sodium borohydride ($NaBH_4$).[21] To optimize the synthetic route for efficient growth of QCs, it is necessary to understand growth process of the same.[27] Knowledge of temporal growth mechanism of QCs helps in the determination of relationships between reaction parameters which facilitate tunability of physicochemical properties of the clusters formed.

To monitor such growth processes of QCs, selection of appropriate techniques are important. For slower growth processes which occur at the time scale of hours and days, methods which would involve complex and lengthy sample preparation methods can be used. These techniques can be transmission electron microscopy (HRTEM), scanning electron microscopy (SEM) or mass spectrometric techniques such as matrix assisted laser desorption ionization mass spectrometry (MALDI MS), etc. But, for reactions which occur at time scale of seconds or minutes, real time probing techniques are required. Depending on the intrinsic properties of products, for solution state synthesis, the techniques can be UV−vis absorption, PL spectroscopy, etc. Dharmaratne et al. have shown that for the growth of monolayer protected QCs, which occurs on the time scale of hours, mass spectrometry can be used.[28] In this study, size evolution of $Au_{25}(SCH_2CH_2Ph)_{18}$

Received: January 17, 2015
Revised: April 15, 2015
Published: April 20, 2015





DOI: 10.1021/acs.jpcc.5b00496
J. Phys. Chem. C 2015, 119, 9988−9994

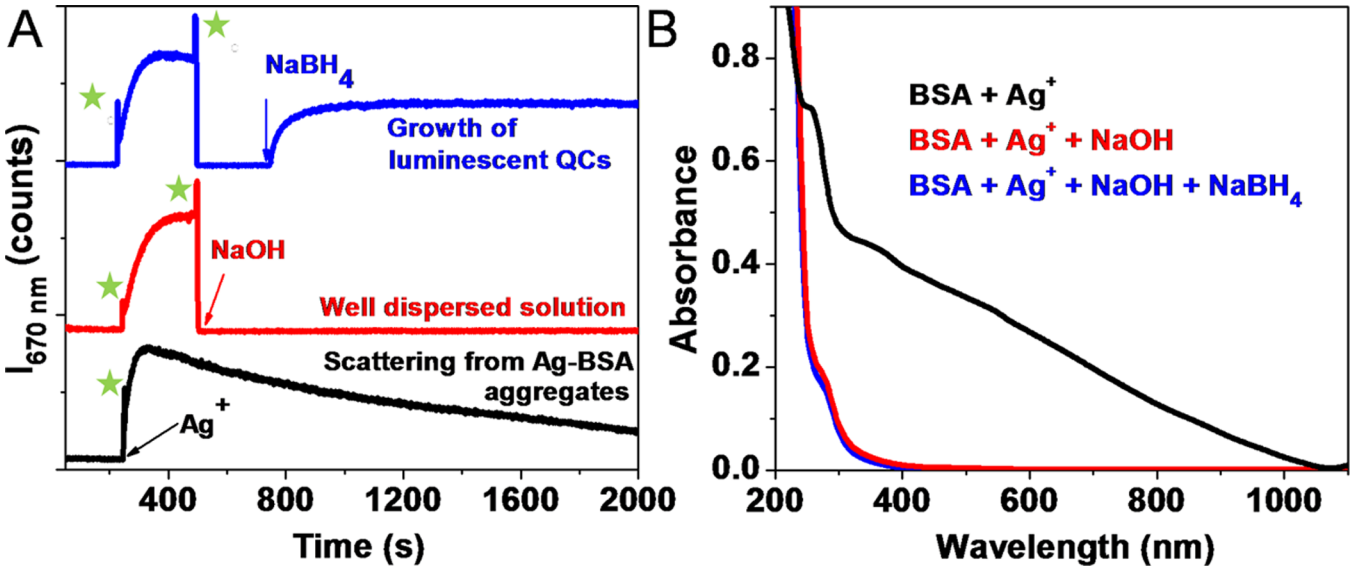


**Figure 1.** Role of NaOH in the AgQC synthesis. (A) Changes in the PL counts ($I_{670}$) after the stepwise addition of various reaction components during AgQC synthesis. The black curve shows variations in $I_{670}$ when only $Ag^+$ ions were added to the BSA solution, and reaction was monitored without adding NaOH and $NaBH_4$. The red curve shows variations in $I_{670}$ when addition of $Ag^+$ was followed by an addition of NaOH. The blue curve shows variations in $I_{670}$ when $Ag^+$, NaOH and $NaBH_4$ were added sequentially. Green stars indicate the occurrence of spikes due to increase in the detector response when stray light got into the spectrometer during the addition of reactants. (B) UV−vis spectra of the aforementioned samples are shown in matching color at 2000 s time of reaction.

nanoclusters was probed using MALDI MS. It was found that initial growth of larger sized clusters such as $Au_{102}$, $Au_{38}$ and $Au_{68}$ leads to the formation of highly monodisperse $Au_{25}$ nanoclusters. Another study, performed by Xie and co-workers, has used ESI-MS to monitor the time evolution of $Au_{25}$ nanoclusters.[29] This study has proposed a two-stage growth process which involves a fast reduction-growth step and a slow intercluster conversion, leading to $Au_{25}$. Our group has also reported monitoring of growth processes of protein protected clusters.[21,27,30,31] Our study on the evolution of AuQCs within lactoferrin templates have shown that during the growth of AuQCs, initial addition of $Au^{3+}$ ions in protein solution lead to its reduction to $Au^+$ which reduces to Au(0) only when the pH is changed to a basic value.[27] This growth process is much slower than the growth process for AgQCs. Growth of AuQCs inside lactoferrin templates involves interprotein metal ion transfer which leads to the emergence of parent protein molecules, at the end of the reaction, beginning from metal-protein adducts. This knowledge obtained from AuQC growth process was used to develop an optimized synthetic route which utilizes the free protein available at the end of reaction. This kind of optimization is mainly necessary when availability of proteins and monodispersity of product are major concerns. A similar phenomenon of the emergence of parent protein was observed when the growth process of AuAg alloy clusters inside BSA templates was monitored.[30] Recent studies from our group have used small-angle X-ray scattering (SAXS) and mass spectrometry (MS) for direct visualization of QC growth within protein templates in solution.[31] In another study, performed by Mathew et al., MALDI MS was used to investigate the effect of $NaBH_4$ on the synthesis of AgQC@BSA.[21] It was found that despite the change in concentration of $NaBH_4$, the major species formed was $Ag_{15}$@BSA.[21] However, as mentioned, due to the use of $NaBH_4$ as the reducing agent for $Ag^+$, growth kinetics of AgQC@protein is much faster as compared to AuQC@protein. Hence, MALDI MS was able to provide information about the final product only. MALDI MS also has another drawback that the clusters may be formed in the gas phase by reaction between desorbed proteins and the naked clusters produced in the gas phase.[5] Hence it is risky to correlate the clusters obtained from MALDI MS with the PL properties of QCs measured in solution, in all cases. Hence, in this work, we have used PL spectroscopy to probe the initial growth kinetics of luminescent AgQC@BSA. Unlike MALDI MS, PL spectroscopy allows real time and direct monitoring of the PL properties of clusters growing in the solution state. The study has been performed mainly to check the dependence of growth kinetics on various reaction parameters when NIR luminescent AgQCs are formed. Dependence of excitation and emission wavelengths on the $NaBH_4$ concentration has been established. Growth process was studied for two albumin family proteins, BSA and Ovalbumin (Ova). To the best of our knowledge, this is the first study on the growth kinetics of rapidly synthesized AgQCs inside protein templates.

## EXPERIMENTAL SECTION

**Chemicals.** Sodium borohydride (99%, Fluka), Ovalbumin (98%, Sigma-Aldrich), Sodium hydroxide (98%, RANKEM, India.), Silver nitrate (99.9%, RANKEM, India.), Bovine serum albumin (96−98%, pH 7, SRL Pvt. Ltd., India.) were used for experiments. Millipore deionized water (DI) (~18.2 MΩ) was used throughout the experiments.

**Synthesis of AgQCs.** A protocol previously reported[21] from our group was used for the synthesis of AgQC@BSA and AgQC@Ova with slight modifications. Briefly, 200 μL of 100 mM $AgNO_3$ was added to 2 mL of 25 mg/mL protein solution followed by the addition of 100 μL of 1 M NaOH. Then, 10 mM $NaBH_4$ was added to initiate cluster growth. Volume of $NaBH_4$ was varied from 5 to 200 μL according to the experiment. While varying $NaBH_4$, final volume of the reaction mixture was maintained constant by adding DI water. No


DOI: 10.1021/acs.jpcc.5b00496
J. Phys. Chem. C 2015, 119, 9988−9994

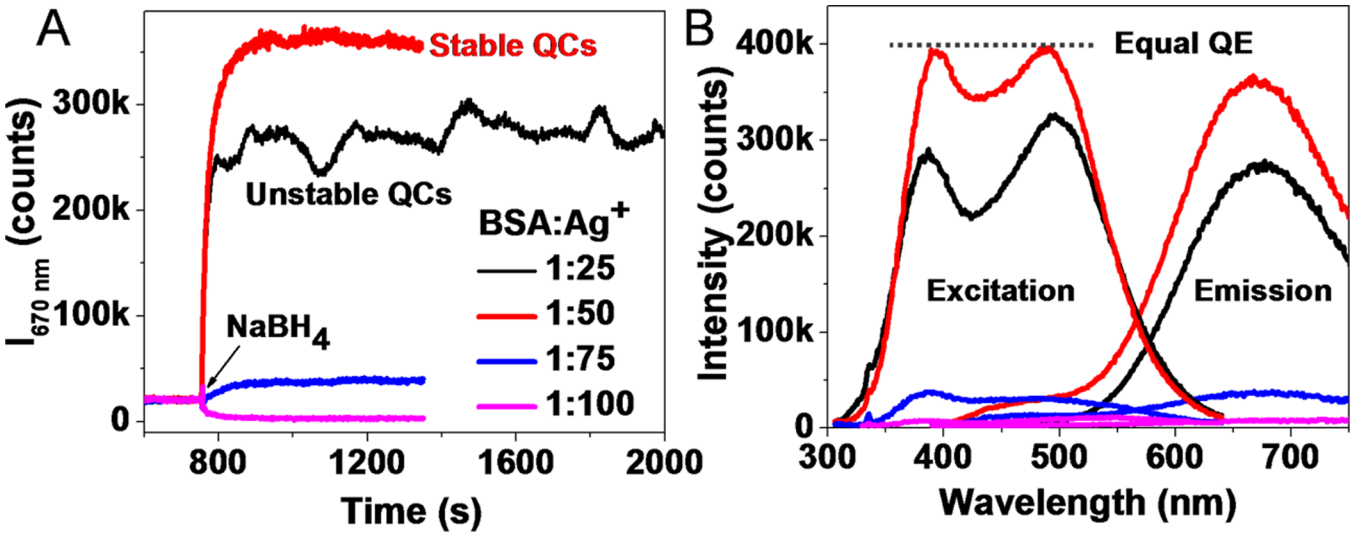


**Figure 2.** Initial growth kinetics of AgQC@BSA at different $Ag^+$ concentrations. (A) Changes in the PL intensity of AgQC@BSA (Ex−380 nm, Em−670 nm) after the addition of $NaBH_4$ at different concentrations of $Ag^+$. (B) Excitation and emission spectra corresponding to the growth curves shown in (A). Colors in B indicate concentrations shown in A. QE stands for quantum efficiency at 670 nm emission.

stirring was used but solution was gently mixed with using 100 $\mu$L pipet.

**PL spectroscopy.** To monitor AgQC growth kinetics in real time, we have carried out reaction in the sample cuvette of PL spectrometer kept within a dark room. HORIBA, JOBIN VYON NanoLog fluorescence spectrometer was used for PL measurements. Protein (BSA or Ova) solution was taken in quartz cuvette and other components were added in the order, $AgNO_3$, NaOH and $NaBH_4$. After an addition of every reactant, sufficient time was given to ensure the stability of PL counts. Final volume of the reaction was kept constant by adding deionized water (DI) to achieve better comparison between PL intensity of different products. Care was taken to avoid second order peak of excitation in emission spectra.

**UV−vis spectroscopy.** UV−visible absorption spectroscopic measurements were performed using PerkinElmer Lambda 25 spectrophotometer (Range -200−1100 nm, scan rate -480 nm per min).

Such clusters were monitored in our earlier studies by a range of techniques such as MALDI MS, XPS, HRTEM, SAXS, etc.[27,31,32] Although data from those studies are not presented, inferences drawn from these studies will be used here.

## RESULTS AND DISCUSSION

**Role of NaOH and $NaBH_4$ in AgQC synthesis.** NIR luminescent AgQC@BSA and AgQC@Ova do not form at neutral pH (Figure 1), and neither do they form only by the addition of NaOH. Previous studies from our group have shown using gas phase mass spectrometric studies that basic pH facilitates coordination between $Ag^+$ ions and various functional groups of BSA.[21] PL spectroscopic observations performed in the solution state have shown the importance of NaOH in this reaction. For these observations, reaction was monitored step by step after the addition of various components of the reaction. The mixture was excited at 380 nm and emission was collected at 670 nm ($I_{670}$). It may be noted that these are the excitation and emission values of AgQC@BSA. As shown in Figure 1, when only $Ag^+$ ions were added to BSA solution, a large increase in $I_{670}$ counts was observed, which decayed slowly over long time. This was found to be due to aggregation of BSA in the presence of $Ag^+$ ions. Soon after the addition of $Ag^+$, solution became turbid white and $I_{670}$ increases, due to scattering. This was supported by UV−vis spectroscopic data as shown in Figure 1B. Subsequent decrease in $I_{670}$ was due to gradual settling down of aggregates. In the next step of the reaction, after the addition of $Ag^+$, it was observed that due to change in the pH of reaction mixture, aggregates break down and form well dispersed solutions of Ag-BSA conjugates.

In this reaction, NaOH does not initiate NIR luminescent AgQC growth even after long time as it can be seen by the red trace shown in Figure 1. This results in an abrupt decrease in $I_{670}$. At this time, it again reaches the baseline counts, which were observed before the addition of $Ag^+$. This baseline count continues for long time without any further change. In the next reaction, addition of $Ag^+$ and NaOH was followed by $NaBH_4$. In this case, $I_{670}$ increases exponentially and reaches a stable count within a few minutes. This time, $I_{670}$ remains steady even after a long time. This suggests stable product formation in the reaction. Hence NaOH provides favorable environment for cluster growth and then $NaBH_4$ helps in the growth of stable clusters. Apart from the reduction of $Ag^+$ to Ag(0), $NaBH_4$ can affect the reaction in various ways such as change in the reaction pH and disruption of protein structure, which facilitates the binding of $Ag^+$ ions to the inner residues of the protein. This suggests that apart from facilitating $Ag^+$-BSA conjugation, the other role of NaOH is to provide a well dispersed solution for cluster growth before the addition of $NaBH_4$ (Figure 1A). We have monitored the same reaction at different concentrations of $Ag^+$. These results are discussed in the next section.

**Initial growth kinetics of AgQC@BSA at different $Ag^+$ concentrations.** According to the first report on the synthesis of AgQC@BSA from our group, 1:13 molar ratio of BSA:$Ag^+$ was needed for the synthesis of $Ag_{15}$@BSA.[21] In this study, even after the addition of large amounts of $NaBH_4$, no considerable change in the emission of QCs was observed. This was possibly because the number of available silver atoms was adequate only for the synthesis of $Ag_{15}$. To understand if changes in the relative quantity of $NaBH_4$ can lead to changes in the cluster growth, at first we have studied growth kinetics


DOI: 10.1021/acs.jpcc.5b00496
J. Phys. Chem. C 2015, 119, 9988−9994

and PL properties at different concentrations of $Ag^+$. In this experiment, $NaBH_4$ (10 mM, 25 $\mu$L) and NaOH (1 M, 100 $\mu$L) concentrations were kept constant, only $Ag^+$ concentration was varied. Growth curves for these samples are shown in Figure 2A. When ~1:25 ratio of BSA:$Ag^+$ was used, stable cluster growth was not observed. Fluctuations in the PL intensity were observed at this concentration. Whereas at higher concentration of $Ag^+$, that is at ~1:50 ratio of BSA:$Ag^+$, the clusters grown were stabilized. For this sample, even higher PL intensity was observed as compared to clusters grown with 1:25 ratio. It should be noted that, despite using similar $NaBH_4$ concentration for 1:50 and 1:25 ratios, only 1:50 forms a stable product. Figure 2B shows steady state PL spectra of these samples. These spectra were collected at a time when growth monitoring was stopped (2000 s). For all samples, only one major emission peak was observed at ~670 nm. First excitation peak at ~376 nm is due to the excitation of Ag-BSA conjugate.[21] Second excitation peak at ~500 nm appears only after $NaBH_4$ addition and due to the excitation of NIR luminescent AgQC@BSA. When stable and highly emissive clusters were formed, both these excitations exhibit equal intensity for emission at 670 nm (Figure 2B). This implies that for 376 and 500 nm excitation wavelengths, AgQC@BSA exhibit equal quantum efficiency (QE). In the absence of NIR luminescent clusters, excitation at 376 nm leads to emission at ~460 nm. It has been shown by previous studies that tryptophan metabolites like kynurenine are responsible for excitation and emission of protein at 375 and 450 nm, respectively.[8,33] At further higher concentrations of $Ag^+$, no NIR luminescent cluster growth was observed. The reason behind this may be the growth of larger size clusters and is discussed in more detail in the subsequent sections with the help of steady state PL spectroscopy of AgQCs.

**Growth kinetics of AgQC@BSA at different $NaBH_4$ concentrations.** Figure 3A shows the growth curves of AgQC@BSA when different volumes of $NaBH_4$ were used to initiate growth of clusters. Figure 3B shows the slopes (growth rates) calculated from the tangents drawn to growth curves just after the addition of $NaBH_4$. Initially at lower concentrations of $NaBH_4$ (5, 10, 25 $\mu$L), growth rate increases as the concentration of $NaBH_4$ increases. To understand the kinetics further, we have tried fitting the growth curves using a single component exponential growth function. Though it was possible to fit curves with the adjusted R square values of ~0.97, no specific correlation between growth constants and $NaBH_4$ concentration was found. These growth constants and description of exponential growth function are provided in Supporting Information Table 1. Because of this, here we have discussed growth curves only qualitatively. From the $I_{670}$ values at 500 s, for clusters grown with different concentrations of $NaBH_4$ (Figure 3B), we see that 25 $\mu$L of $NaBH_4$ leads to efficient and stable growth of AgQCs. Further addition of $NaBH_4$ does not result in change of growth rate but after initial transient growth, formation of nonluminescent clusters dominate the growth of luminescent QCs (Figure 3B). After adding 50 $\mu$L of $NaBH_4$, QC growth follows a step function; where just after the addition of $NaBH_4$, clusters grow abruptly and the concentration remains stable even after long time. This difference between growth curves for 25 and 50 $\mu$L concentrations of $NaBH_4$ suggests that, at lower concentration (25 $\mu$L) of $NaBH_4$, although clusters start nucleating at high growth rate, after a few seconds, silver atom uptake by the protein is slow. This leads to QC growth in a controlled

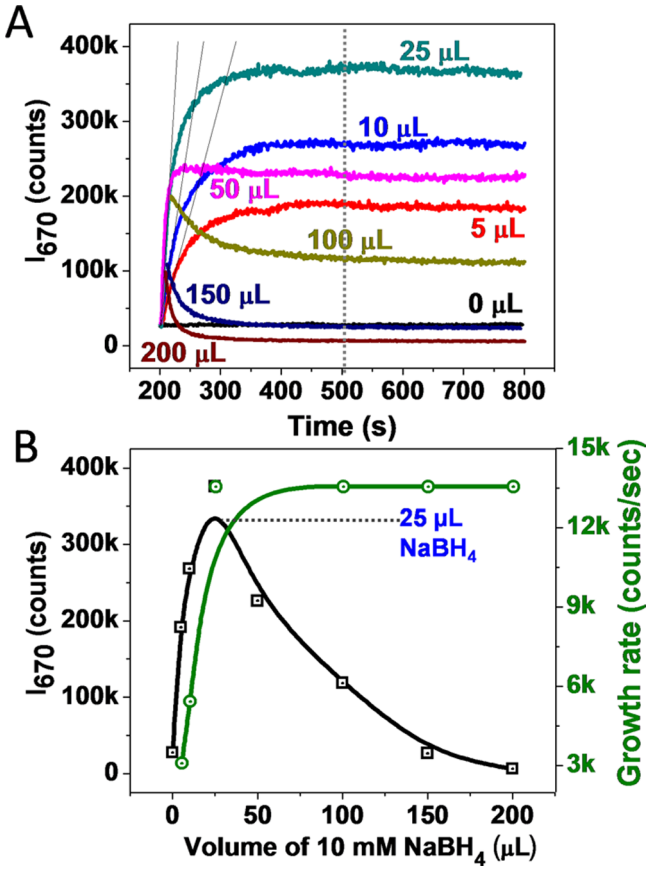


**Figure 3.** Growth kinetics of AgQC@BSA at different concentrations of $NaBH_4$. (A) Changes in the PL intensity of AgQC@BSA (Ex−380 nm, Em−670 nm) after the addition of $NaBH_4$ (10 mM). The volume of $NaBH_4$ added is written adjacent to the growth curves in corresponding colors. Tangents are drawn to determine initial growth rate at different concentrations of $NaBH_4$. The dotted line crosses the data points which are plotted in the next figure. (B) The black curve shows changes in the emission intensity of AgQC@BSA after the addition of different amounts of $NaBH_4$ after 500 s of the reaction. The green curve shows changes in the growth rate of AgQC@BSA.

manner. Whereas, in the case of 50 $\mu$L $NaBH_4$, formation of larger and nonluminescent QCs dominate the nucleation of luminescent QCs soon after the addition of $NaBH_4$. At further higher concentrations of $NaBH_4$, growth of larger QCs leads to reduction in $I_{670}$. Formation of larger clusters was confirmed by red shift observed in steady state PL spectra of aforementioned samples. These observations are discussed in the next section.

**Relationship between PL properties of AgQC@BSA and $NaBH_4$ concentration.** Figure 4A shows excitation spectra of AgQC@BSA grown with different concentrations of $NaBH_4$. In all these spectra, we see that the excitation peak for Ag-BSA conjugate ($Ex_{380}$) appears even before the addition of $NaBH_4$ (black trace at the bottom of Figure 4A). $Ex_{380}$ remains constant in position but changes in intensity upon change in the concentration of $NaBH_4$. But the excitation peak in the region around 500 nm ($\lambda_{ex}$) changes in position and intensity, which is attributed to different QCs nucleated in the solution. For 25 $\mu$L of $NaBH_4$ concentration, both $Ex_{380}$ and $\lambda_{ex}$ can be used to excite AgQC@BSA with equal quantum efficiency for emission at 670 nm. But, after increase in the concentration of $NaBH_4$, there are corresponding changes in the PL properties of QCs too. Assuming that larger quantum clusters have longer


DOI: 10.1021/acs.jpcc.5b00496
J. Phys. Chem. C 2015, 119, 9988−9994

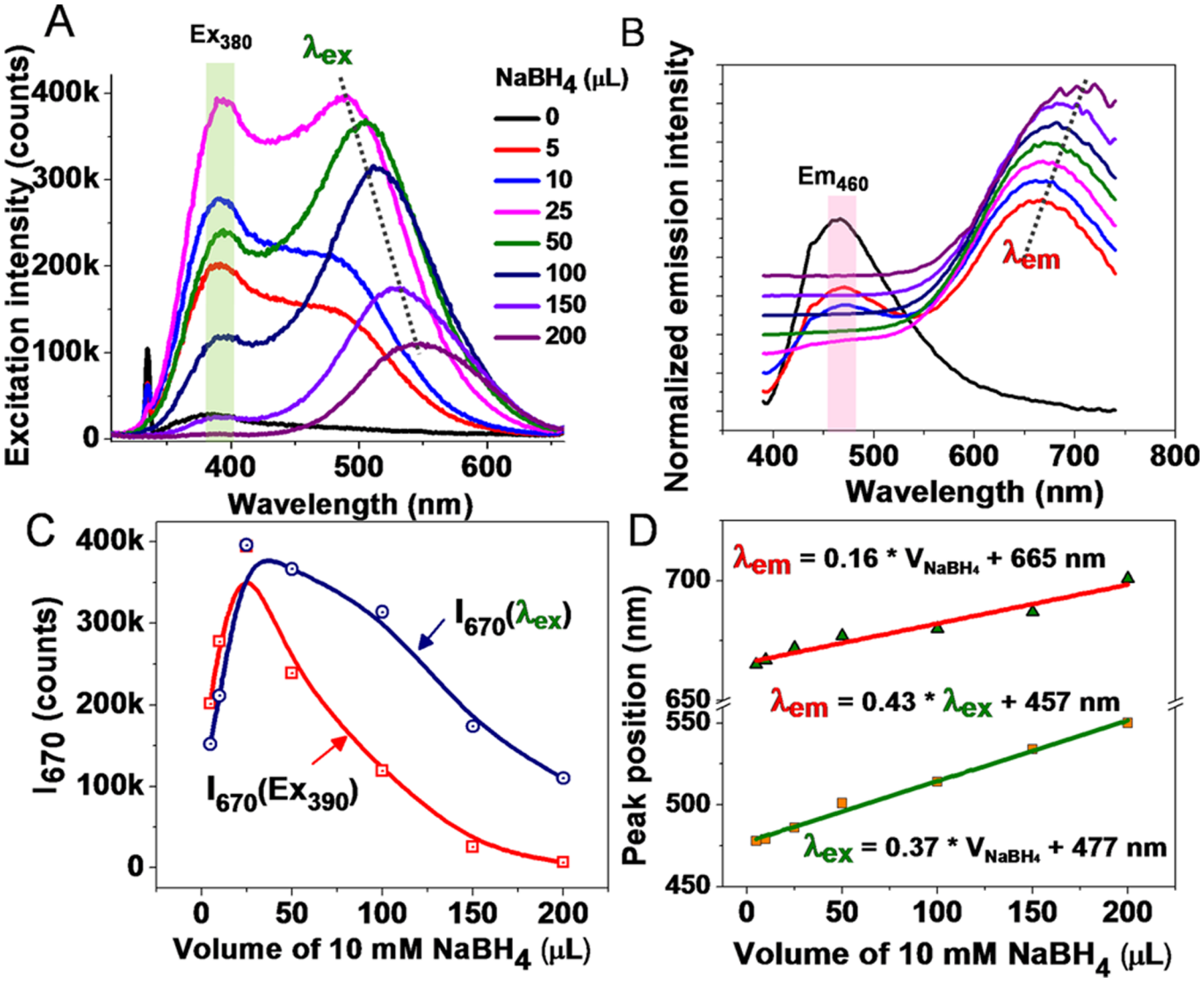


**Figure 4.** Relationship between PL properties of AgQC@BSA and $NaBH_4$ concentration. (A) Excitation spectra (Em−670 nm) of AgQC@BSA. (B) Emission spectra (Ex−380 nm) of AgQC@BSA. Matching colors are used for excitation and emission. Emission spectra are normalized and vertically translated for better comparison of peak positions. (C) Changes in $I_{670}$ as a function of $NaBH_4$ concentration shown for two different excitations, $\lambda_{ex}$ (blue) and $Ex_{380}$ (red). (D) Relationships between excitation ($\lambda_{ex}$) and emission ($\lambda_{em}$) wavelengths and volume of $NaBH_4$ ($V_{NaBH4}$) are shown.

excitation wavelength, uniform red-shift in $\lambda_{ex}$ can be attributed to an increase in the size of clusters. Such red-shift in the cluster emission has also been shown by Petty *et. al* and Gwinn et al. for DNA templated AgQCs.[34,35] In the emission spectra also, $Em_{460}$ remains constant but cluster emission ($\lambda_{em}$) exhibits a red shift. Hence, due to red shift, $\lambda_{ex}$ gradually goes out of $Em_{460}$ range and results in a decrease in the efficiency of $Ex_{380}$.

To compare the excitation and emission peak positions accurately, we have done Gaussian curve fitting of all the excitation and emission spectra. Curve fitting data are shown in Supporting Information Figures S2 and S3. Peak positions obtained from these fittings are plotted in Figure 4D. It was observed that both excitation and emission wavelengths scale linearly with respect to the volume of $NaBH_4$ ($V_{NaBH4}$). The slope values of 0.37 and 0.16 for $\lambda_{ex}$ and $\lambda_{em}$ suggest that, excitation is more a prominent function of $NaBH_4$ concentration as compared to emission. This also implies linear relationship between the excitation and emission of clusters synthesized at different volumes of $NaBH_4$. To check the possibility of similar behavior in other AgQC@protein systems, we have performed similar studies on another system of AgQCs stabilized by Ovalbumin (AgQC@Ova). These results are discussed in the next section.

**Growth kinetics of AgQC@Ova.** To confirm the observations made for AgQC@BSA and to verify whether this behavior can be generalized for other albumin family proteins, we have monitored growth kinetics of AgQC@Ova. Before discussing these observations, it should be noted that molecular weight (MW) and hence amino acid content of Ova is ~2/3 of BSA. Hence these observations can also be used for such MW based comparison. Hence keeping the weight/volume concentration of Ova the same as BSA, $NaBH_4$ concentration was varied. Results obtained are consolidated in Figure 5. Similar to AgQC@BSA, initial growth rate of AgQC@Ova increases upon increase in the concentration of $NaBH_4$ and remains constant at an optimum concentration (Supporting Information Figure S6). In the case of AgQC@Ova also, 50 $\mu$L concentration of $NaBH_4$ leads to a growth curve similar to a step function and clusters grow abruptly after the addition of $NaBH_4$. Figure 5B shows linear relationships


DOI: 10.1021/acs.jpcc.5b00496
J. Phys. Chem. C 2015, 119, 9988−9994

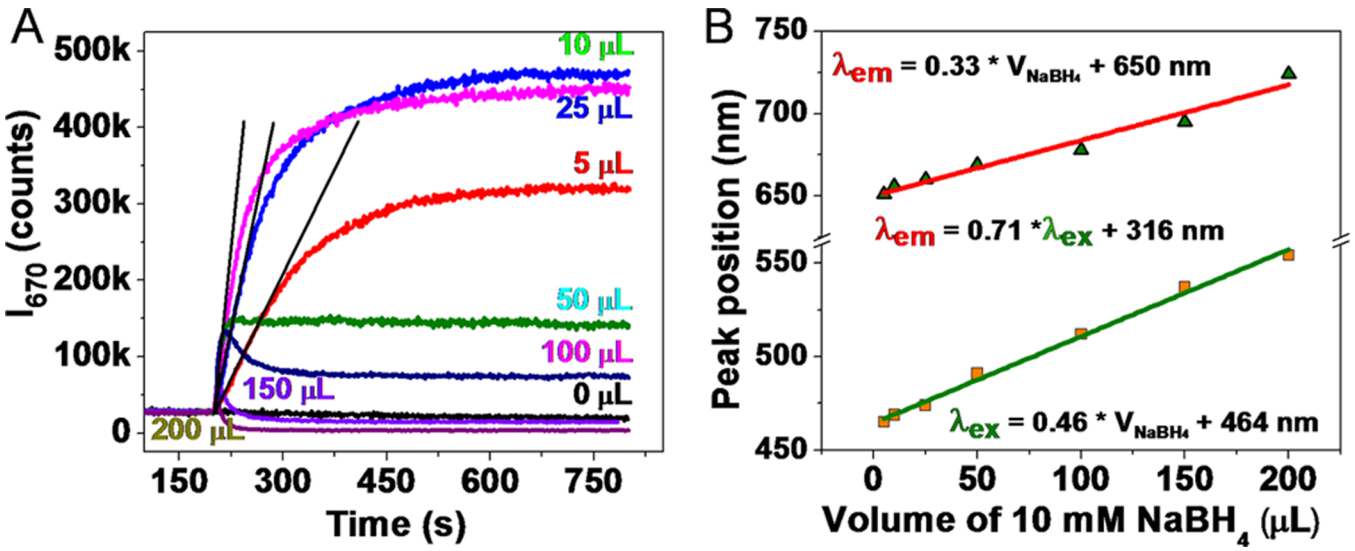


**Figure 5.** Growth kinetics and PL spectroscopy of AgQC@Ova. (A) Changes in the PL intensity of AgQC@Ova (Ex−380 nm, Em−670 nm) after the addition of $NaBH_4$. Tangents are drawn to determine initial growth rate at different volumes of 10 mM $NaBH_4$. (B) Relationships between excitation and emission wavelengths and volume of $NaBH_4$ are shown.

between excitation, emission and concentration of $NaBH_4$. Original excitation and emission spectra for these samples are shown in Supporting Information Figure S1 and curve fitting data are shown in Figures S4 and S5. This supports that, the kinetics of AgQC growth inside BSA and Ova can be considered as a generalized kinetics for albumin family proteins. PL data also suggest that Ova provides more tunability over emission (Em = 650−720 nm) as compared to BSA (Em = 660−700 nm).

Unlike gold quantum clusters, for which jellium model has been developed to correlate emission energy with the number of atoms per clusters,[36,37] for the case of silver clusters, due to the strongly interacting ligands to stabilize cluster core, such a model is unlikely to be followed. However, there have been attempts to apply jellium model for silver-protein nanobioconjugates.[38] If such a model were to be applied in the present study, sizes of AgQCs would have been 24−28 atoms for BSA emission varying between 660 and 700 nm and 23−31 atoms per cluster for Ova emission varying from 650 to 720 nm (Supporting Information Figure S7).

UV−vis spectra of AgQC@BSA and AgQC@Ova do not yield any conclusive information to enlighten the growth process. The possible reasons behind this can be the lack of surface plasmon resonance due to the ultrasmall size of quantum clusters as well as the bulky nature of the protein ligands and their high absorption which may hide the absorption features of the clusters. UV−vis spectra of AgQC@BSA and AgQC@Ova spectra are shown in Supporting Information Figures S8 and S9.

## CONCLUSION

We have developed a methodology for monitoring real time growth kinetics of rapidly synthesized luminescent silver quantum clusters. This method allows understanding as well as precise optimization of the synthetic methodology. With the example of AgQC@BSA, we have shown that upon increase in the concentration of $NaBH_4$, the growth rate of luminescent AgQCs increases and becomes constant for concentrations higher than the optimum value. Studies performed at different concentrations of $Ag^+$ have shown that merely the addition of more $NaBH_4$ does not lead to stable cluster growth, but sufficient concentration of $Ag^+$ is also an important parameter. Steady state PL spectroscopic investigations have shown that excitation and emission properties of clusters are linear functions of $NaBH_4$ concentration. Similar relationships were observed for both the proteins, Ova, and BSA.

This study also provides a new possibility of using AgQC@BSA as probes for multiple labeling or detection using the ratiometric fluorescence technique. Further probing of this system with advanced techniques and other methodologies may be required to answer questions such as reasons behind the increased tunability of AgQCs by Ova as compared to BSA, larger red-shift in the excitation wavelength of QCs compared to red-shift in the emission, etc. We believe that this study will be helpful for further improvements in the synthetic methodology and applications of protein protected AgQCs.

## ASSOCIATED CONTENT

### Supporting Information

Excitation and emission spectra of the systems described, spectra after appropriate peak fitting under various conditions, and a table of growth constants derived from the exponential fitting of spectra. The Supporting Information is available free of charge on the ACS Publications website at DOI: 10.1021/acs.jpcc.5b00496.

## AUTHOR INFORMATION

### Corresponding Author

*E-mail: pradeep@iitm.ac.in.

### Notes

The authors declare no competing financial interest.

## ACKNOWLEDGMENTS

We thank the Department of Science and Technology, Government of India, for constantly supporting our research program on nanomaterials.



DOI: 10.1021/acs.jpcc.5b00496
J. Phys. Chem. C 2015, 119, 9988−9994

## REFERENCES


(1) Xavier, P. L.; Chaudhari, K.; Baksi, A.; Pradeep, T. Protein-Protected Luminescent Noble Metal Quantum Clusters: An Emerging Trend in Atomic Cluster Nanoscience. *Nano Rev.* **2012**, *3*, 14767.

(2) Wei, H.; Wang, Z.; Yang, L.; Tian, S.; Hou, C.; Lu, Y. Lysozyme-Stabilized Gold Fluorescent Cluster: Synthesis and Application as $Hg^{2+}$ Sensor. *Analyst* **2010**, *135*, 1406−1410.

(3) Ghosh, R.; Sahoo, A. K.; Ghosh, S. S.; Paul, A.; Chattopadhyay, A. Blue-Emitting Copper Nanoclusters Synthesized in the Presence of Lysozyme as Candidates for Cell Labeling. *ACS Appl. Mater. Interfaces* **2014**, *6*, 3822−8.

(4) Liu, C.-L.; et al. Insulin-Directed Synthesis of Fluorescent Gold Nanoclusters: Preservation of Insulin Bioactivity and Versatility in Cell Imaging. *Angew. Chem., Int. Ed.* **2011**, *50*, 7056−7060.

(5) Baksi, A.; Pradeep, T. Noble Metal Alloy Clusters in the Gas Phase Derived from Protein Templates: Unusual Recognition of Palladium by Gold. *Nanoscale* **2013**, *5*, 12245−12254.

(6) Luo, Z.; Zheng, K.; Xie, J. Engineering Ultrasmall Water-Soluble Gold and Silver Nanoclusters for Biomedical Applications. *Chem. Commun.* **2014**, *50*, 5143−5155.

(7) Antoku, Y.; Hotta, J.-I.; Mizuno, H.; Dickson, R. M.; Hofkens, J.; Vosch, T. Transfection of Living Hela Cells with Fluorescent Poly-Cytosine Encapsulated Ag Nanoclusters. *Photochemical & Photobiological Sciences* **2010**, *9*, 716−721.

(8) Goswami, N.; Giri, A.; Bootharaju, M. S.; Xavier, P. L.; Pradeep, T.; Pal, S. K. Copper Quantum Clusters in Protein Matrix: Potential Sensor of $Pb^{2+}$ Ion. *Anal. Chem.* **2011**, *83*, 9676−80.

(9) Goswami, N.; Giri, A.; Kar, S.; Bootharaju, M. S.; John, R.; Xavier, P. L.; Pradeep, T.; Pal, S. K. Protein-Directed Synthesis of NIR-Emitting, Tunable HgS Quantum Dots and Their Applications in Metal-Ion Sensing. *Small* **2012**, *8*, 3175−3184.

(10) Durgadas, C. V.; Sharma, C. P.; Sreenivasan, K. Fluorescent Gold Clusters as Nanosensors for Copper Ions in Live Cells. *Analyst* **2011**, *136*, 933−940.

(11) Retnakumari, A.; Setua, S.; Menon, D.; Ravindran, P.; Muhammed, H.; Pradeep, T.; Nair, S.; Koyakutty, M. Molecular-Receptor-Specific, Non-Toxic, Near-Infrared-Emitting Au Cluster-Protein Nanoconjugates for Targeted Cancer Imaging. *Nanotechnology* **2010**, *21*, 055103.

(12) Zhang, X. D.; Wu, D.; Shen, X.; Liu, P. X.; Fan, F. Y.; Fan, S. J. In Vivo Renal Clearance, Biodistribution, Toxicity of Gold Nanoclusters. *Biomaterials* **2012**, *33*, 4628−4638.

(13) Retnakumari, A.; Jayasimhan, J.; Chandran, P.; Menon, D.; Nair, S.; Mony, U.; Koyakutty, M. CD33 Monoclonal Antibody Conjugated Au Cluster Nano-Bioprobe for Targeted Flow-Cytometric Detection of Acute Myeloid Leukaemia. *Nanotechnology* **2011**, *22*, 285102.

(14) Wang, M.; Mei, Q.; Zhang, K.; Zhang, Z. Protein-Gold Nanoclusters for Identification of Amino Acids by Metal Ions Modulated Ratiometric Fluorescence. *Analyst* **2012**, *137*, 1618−1623.

(15) Wen, Q.; Gu, Y.; Tang, L. J.; Yu, R. Q.; Jiang, J. H. Peptide-Templated Gold Nanocluster Beacon as a Sensitive, Label-Free Sensor for Protein Post-Translational Modification Enzymes. *Anal. Chem.* **2013**, *85*, 11681−11685.

(16) Gu, Y.; Wen, Q.; Kuang, Y.; Tang, L.; Jiang, J. Peptide-Templated Gold Nanoclusters as a Novel Label-Free Biosensor for the Detection of Protease Activity. *RSC Adv.* **2014**, *4*, 13753−13756.

(17) Chattoraj, S.; Bhattacharyya, K. Fluorescent Gold Nanocluster inside a Live Breast Cell: Etching and Higher Uptake in Cancer Cell. *J. Phys. Chem. C* **2014**, *118*, 22339−22346.

(18) Xavier, P. L.; Chaudhari, K.; Verma, P. K.; Pal, S. K.; Pradeep, T. Luminescent Quantum Clusters of Gold in Transferrin Family Protein, Lactoferrin Exhibiting Fret. *Nanoscale* **2010**, *2*, 2769−2776.

(19) Kawasaki, H.; Hamaguchi, K.; Osaka, I.; Arakawa, R. pH-Dependent Synthesis of Pepsin-Mediated Gold Nanoclusters with Blue Green and Red Fluorescent Emission. *Adv. Funct. Mater.* **2011**, *21*, 3508−3515.

(20) Le Guevel, X.; Hotzer, B.; Jung, G.; Hollemeyer, K.; Trouillet, V.; Schneider, M. Formation of Fluorescent Metal (Au, Ag) Nanoclusters Capped in Bovine Serum Albumin Followed by Fluorescence and Spectroscopy. *J. Phys. Chem. C* **2011**, *115*, 10955−10963.

(21) Mathew, A.; Sajanlal, P. R.; Pradeep, T. A Fifteen Atom Silver Cluster Confined in Bovine Serum Albumin. *J. Mater. Chem.* **2011**, *21*, 11205−11212.

(22) Baksi, A.; Xavier, P. L.; Chaudhari, K.; Goswami, N.; Pal, S. K.; Pradeep, T. Protein-Encapsulated Gold Cluster Aggregates: The Case of Lysozyme. *Nanoscale* **2013**, *5*, 2009−2016.

(23) Petty, J. T.; Fan, C.; Story, S. P.; Sengupta, B.; Sartin, M.; Hsiang, J. C.; Perry, J. W.; Dickson, R. M. Optically Enhanced, Near-IR, Silver Cluster Emission Altered by Single Base Changes in the DNA Template. *J. Phys. Chem. B* **2011**, *115*, 7996−8003.

(24) Xie, J.; Zheng, Y.; Ying, J. Y. Protein-Directed Synthesis of Highly Fluorescent Gold Nanoclusters. *J. Am. Chem. Soc.* **2009**, *131*, 888−889.

(25) Habeeb Muhammed, M. A.; Verma, P. K.; Pal, S. K.; Retnakumari, A.; Koyakutty, M.; Nair, S.; Pradeep, T. Luminescent Quantum Clusters of Gold in Bulk by Albumin-Induced Core Etching of Nanoparticles: Metal Ion Sensing, Metal-Enhanced Luminescence, and Biolabeling. *Chem.—Eur. J.* **2010**, *16*, 10103−10112.

(26) Yu, Y.; Chen, X.; Yao, Q.; Yu, Y.; Yan, N.; Xie, J. Scalable and Precise Synthesis of Thiolated Au10−12, Au15, Au8, and Au25 Nanoclusters Via pH Controlled Co Reduction. *Chem. Mater.* **2013**, *25*, 946−952.

(27) Chaudhari, K.; Xavier, P. L.; Predeep, T. Understanding the Evolution of Luminescent Gold Quantum Clusters in Protein Templates. *ACS Nano* **2011**, *5*, 8816−8827.

(28) Dharmaratne, A. C.; Krick, T.; Dass, A. Nanocluster Size Evolution Studied by Mass Spectrometry in Room Temperature Au25(SR)18 Synthesis. *J. Am. Chem. Soc.* **2009**, *131*, 13604−13605.

(29) Luo, Z.; Nachammai, V.; Zhang, B.; Yan, N.; Leong, D. T.; Jiang, D. E.; Xie, J. Toward Understanding the Growth Mechanism: Tracing All Stable Intermediate Species from Reduction of Au(I)-Thiolate Complexes to Evolution of Au25 Nanoclusters. *J. Am. Chem. Soc.* **2014**, *136*, 10577−10580.

(30) Mohanty, J. S.; Xavier, P. L.; Chaudhari, K.; Bootharaju, M. S.; Goswami, N.; Pal, S. K.; Pradeep, T. Luminescent, Bimetallic Auag Alloy Quantum Clusters in Protein Templates. *Nanoscale* **2012**, *4*, 4255−4262.

(31) Baksi, A.; Mitra, A.; Mohanty, J. S.; Lee, H.; De, G.; Pradeep, T. Size Evolution of Protein-Protected Gold Clusters in Solution: A Combined SAXS-MS Investigation. *J. Phys. Chem. C* **2015**, *119*, 2148−2157.

(32) Chakraborty, I.; Govindarajan, A.; Erusappan, J.; Ghosh, A.; Pradeep, T.; Yoon, B.; Whetten, R. L.; Landman, U. The Superstable 25 Kda Monolayer Protected Silver Nanoparticle: Measurements and Interpretation as an Icosahedral Ag152(SCH2CH2PH)60 Cluster. *Nano Lett.* **2012**, *12*, 5861−5866.

(33) Goswami, N.; Makhal, A.; Pal, S. K. Toward an Alternative Intrinsic Probe for Spectroscopic Characterization of a Protein. *J. Phys. Chem. B* **2010**, *114*, 15236−15243.

(34) Petty, J. T.; Zheng, J.; Hud, N. V.; Dickson, R. M. DNA-Templated Ag Nanocluster Formation. *J. Am. Chem. Soc.* **2004**, *126*, 5207−5212.

(35) Gwinn, E.; Schultz, D.; Copp, S.; Swasey, S. DNA-Protected Silver Clusters for Nanophotonics. *Nanomaterials* **2015**, *5*, 180−207.

(36) Zheng, J.; Zhang, C.; Dickson, R. M. Highly Fluorescent, Water-Soluble, Size-Tunable Gold Quantum Dots. *Phys. Rev. Lett.* **2004**, *93*, 077402.

(37) Zheng, J.; Nicovich, P. R.; Dickson, R. M. Highly Fluorescent Noble-Metal Quantum Dots. *Annu. Rev. Phys. Chem.* **2007**, *58*, 409−431.

(38) Narayanan, S. S.; Pal, S. K. Structural and Functional Characterization of Luminescent Silver−Protein Nanobioconjugates. *J. Phys. Chem. C* **2008**, *112*, 4874−4879.




DOI: 10.1021/acs.jpcc.5b00496
*J. Phys. Chem. C* 2015, 119, 9988−9994